Geoscience Frontiers 7 (2016) 543–553

HOSTED BY

Contents lists available at ScienceDirect

China University of Geosciences (Beijing)

Geoscience Frontiers

journal homepage: www.elsevier.com/locate/gsf

Focus paper

A great thermal divergence in the mantle beginning 2.5 Ga: Geochemical constraints from greenstone basalts and komatiites

Kent C. Condie [a,*], Richard C. Aster [b], Jeroen van Hunen [c]

[a] Department of Earth and Environmental Science, New Mexico Tech, Socorro, NM 87801, USA
[b] Geosciences Department, Colorado State University, Fort Collins, CO 80523, USA
[c] Department of Earth Sciences, University of Durham, Durham DH1 3LE, UK

ARTICLE INFO

Article history:
Received 17 November 2015
Received in revised form
12 January 2016
Accepted 15 January 2016
Available online 2 February 2016

Keywords:
Archean greenstones
Mantle thermal evolution
Basalts
Mantle geochemistry
Komatiites

ABSTRACT

Greenstone basalts and komatiites provide a means to track both mantle composition and magma generation temperature with time. Four types of mantle are characterized from incompatible element distributions in basalts and komatiites: depleted, hydrated, enriched and mantle from which komatiites are derived. Our most important observation is the recognition for the first time of what we refer to as a *Great Thermal Divergence* within the mantle beginning near the end of the Archean, which we ascribe to thermal and convective evolution. Prior to 2.5 Ga, depleted and enriched mantle have indistinguishable thermal histories, whereas at 2.5–2.0 Ga a divergence in mantle magma generation temperature begins between these two types of mantle. Major and incompatible element distributions and calculated magma generation temperatures suggest that Archean enriched mantle did not come from mantle plumes, but was part of an undifferentiated or well-mixed mantle similar in composition to calculated primitive mantle. During this time, however, high-temperature mantle plumes from dominantly depleted sources gave rise to komatiites and associated basalts. Recycling of oceanic crust into the deep mantle after the Archean may have contributed to enrichment of Ti, Al, Ca and Na in basalts derived from enriched mantle sources. After 2.5 Ga, increases in $Mg^{\#}$ in basalts from depleted mantle and decreases in Fe and Mn reflect some combination of growing depletion and cooling of depleted mantle with time. A delay in cooling of depleted mantle until after the Archean probably reflects a combination of greater radiogenic heat sources in the Archean mantle and the propagation of plate tectonics after 3 Ga.

1. Introduction

To address the question of if and when Earth evolved from a stagnant lid to a plate tectonic regime, it is important to have an understanding of the chemical (Hofmann, 1988; Condie, 1994; Herzberg, 1995; Campbell, 2002) and thermal history of the planet (Davies, 2007; Labrosse and Jaupart, 2007; Nakagawa and Tackley, 2012; Van Hunen and Moyen, 2012; Hoink et al., 2013; Korenaga, 2013). A stagnant lid regime exists today on the Moon, Mars and probably on Venus, and is characterized by conductive and heat-pipe volcanic heat loss through a "one-plate" lithosphere. Although numerous papers have been published on this topic, we still have important outstanding questions. One issue not addressed is the compositional and thermal history of different types of mantle. Today we know that the mantle beneath ocean ridges is considerably cooler than the mantle source for oceanic island basalts such as Hawaii (Herzberg et al., 2007; Lee et al., 2009). Furthermore, geochemical and isotopic studies indicate the existence of several compositional reservoirs in the mantle (Hofmann, 1988). To better understand the thermal and tectonic history of the mantle, we must track these reservoirs through time.

One approach to this problem is to use basalts and komatiites, which are produced in the mantle and carry information on the thermal and compositional properties of their sources (Condie, 1994; Hofmann, 1997). Furthermore, these rocks occur in greenstones, which allow us to track these properties of the mantle to at least 3.8 Ga (Abbott et al., 1994; Herzberg et al., 2010). In this study, we make use of an extensive database of well-dated greenstone basalts and komatiites to track through time major element and mantle magma generation temperature (T_g) of oceanic mantle

* Corresponding author.
E-mail address: kcondie@nmt.edu (K.C. Condie).
Peer-review under responsibility of China University of Geosciences (Beijing).

http://dx.doi.org/10.1016/j.gsf.2016.01.006

domains. Incompatible trace element distributions are discussed in previous studies (Condie, 1994, 2003, 2015). Depleted mantle (DM) is sampled today by ocean ridge basalts and has an average mantle magma generation temperature (T_g) of 1350–1380 °C; enriched mantle (EM) is sampled at hot spots and has a T_g of 1450–1500 °C; komatiites are sampled in the Phanerozoic at only one location (Gorgona Island 90 Ma) and may come from plume tails with temperatures near 1600 °C (Campbell et al., 1989); and the fourth type of mantle, hydrated mantle (HM) characterizes convergent plate margins and has a present-day T_g similar to DM. The tectonic settings and mantle sources of modern oceanic basalts can be tracked with some degree of certainty to at least 2.2 Ga. The tight grouping of incompatible element ratios of non-hydrated mantle basalts ≥2.5 Ga suggests the mantle was well mixed by the late Archean (Condie, 2015).

The most exciting result of this study is that for the first time, we are able to track both thermal and compositional properties of depleted and enriched mantle through time and show that a great divergence in these properties occurred soon after the end of the Archean.

2. Methods

We limit our definition of basalt to samples with MgO of 7–17 wt.% and SiO_2 of 45–55 wt.% and komatiites are restricted to MgO of 17–35 wt.%, the upper limit imposed to eliminate rocks that may contain cumulus olivine. Using a smaller MgO range for komatiites (i.e., 20–30 wt.%) does not significantly change the median values upon which our interpretations are based. We group modern oceanic mantle into three categories (depleted (DM), enriched (EM), and hydrated (HM) mantle) based of a combination of geologic and incompatible element characteristics of greenstone basalts as summarized in Condie (2015, 1994) and to this we have added a fourth category, mantle sampled by komatiites (KM), which is rarely sampled after the end of the Archean (Arndt et al., 2008). These geochemical domains are hypothetical end members and as recorded by modern basalts and komatiites (Hart, 1988; Hofman, 1997; Stracke, 2012) and listed in the previous paragraph. The details of how each of these mantle domains is defined are given in Condie (2015) and are not repeated here. Also as discussed by Condie (2015), these mantle domains may exist in stagnant lid planets, and hence tracking them into the Archean and Hadean on Earth may not be equivalent to tracking plate tectonics on Earth into these early time periods. Below we discuss the major element characteristics of the basalts and komatiites through time and how they relate to mantle source compositions. Major element distributions are important in that they track (1) the degree of melting of mantle sources, and (2) the degree of depletion (with elements such as Ti) of the source with time. However, these changes may not track tectonic regimes prior to 2.5 Ga if Earth transitioned into a stagnant lid regime during this time (Van Hunen and Moyen, 2012; Condie, 2015).

Major elements are also used to calculate mantle magma generation temperatures (T_g) using the methods described in Lee et al. (2009). Because our approach in calculating primary magma compositions requires a reverse fractionation correction, samples were first filtered to include only those basalts with MgO of 7–17 wt.% in order to minimize the extent of fractional crystallization. We also eliminated samples that may contain cumulus minerals (chiefly olivine) as reported in the original publications. The primary magma composition is estimated by incrementally adding equilibrium olivine back into the magma, assuming Fe^{2+}/Mg exchange relationship as detailed in Herzberg and Asimow (2008), and Lee et al. (2009). This assumes that the magmas were saturated in olivine, not along a cotectic or with other phases. Selecting magmas with MgO of 7–17 wt.% minimizes these problems, but issues still remain for magmas undergoing pyroxene fractionation or derivation from pyroxenite sources. For the former, we use the filter based on Ca from Herzberg et al. (2007) and Herzberg and Asimow (2008), and for the latter, we select only samples with Fe/Mn ratios between 50 and 60. We terminate olivine addition when the olivine composition reaches a forsterite (Fo) content of 91. Magmas are assumed to be relatively un-oxidized, so an atomic Fe^{3+}/Fe^{T} of 0.1 is assumed. We recognize that there are different approaches to estimating primary magma composition. There is no doubt some uncertainty in assuming a fixed final forsterite content because this quantity varies with the extent of melting; our approach over-estimates temperatures if melting degrees are lower and under-estimates if melting degrees are higher than implied. Herzberg et al. (2007) simultaneously solved for temperature and melting degree in an attempt to reduce the arbitrariness of assuming a final forsterite content. Putirka (2005) used the same approach as ours, but chooses to terminate olivine addition at the highest forsterite content observed; this approach assumes that the magma is in equilibrium with the most depleted mantle residuum, but most magmas represent aggregate polybaric liquids so the average composition of the residues is more appropriate. There are thus inherent, but poorly constrained biases in each of these approaches and it is not clear whether any approach is superior. What we have done is to apply our approach consistently for all samples in order to evaluate whether any robust secular trends in temperature exist. The effects of variations in source composition, cotectic crystallization, magma mixing, and recharge (Lee and Bachmann, 2014) yield uncertainties in primary magma composition greater than our assumption of final forsterite content.

Temperatures of the primary magmas are estimated using MgO and SiO_2 thermobarometry following Lee et al. (2009). Considering all of the sources of error in the calculations, we consider the uncertainty range of our temperature calculations of ±50–100 °C. Because of difficulties in estimating equilibrium olivine composition and identifying samples with cumulus olivine, we do not calculate T_g for komatiites, but rather use published data of from Herzberg et al. (2007) and Herzberg and Asimow (2008). More detailed discussion of uncertainties of temperature calculations is given in Herzberg et al. (2007) and Lee et al. (2009).

Our calculated magma generation temperatures and pressures most likely represent an average temperature and pressure of pooled melts generated by decompression melting and therefore, reflect the average melting conditions in the mantle source. Strictly speaking, these temperatures do not correspond exactly to the mantle potential temperature (T_p) because latent heat absorption during adiabatic decompression melting causes a slight temperature decrease relative to the solid mantle adiabat. However, given the uncertainties in correcting for latent heat release, making this correction is not justified. For a low degree of melting (10–20%), the difference between melting temperatures and the solid mantle adiabat are small (<30 °C), and the differences between the melting temperatures and magma generation temperature are even smaller. For high degree melts (>30%), however, melting temperatures may under-estimate magma generation temperature by ≥100 °C.

3. Results

3.1. Major element distributions

Filtering our geochemical database for alteration and extensive fractional crystallization eliminated 40% of the basalts (from 5669 to 3414 samples) and 66% of the komatiites (from 3267 to 1118 samples). The filtered database with calculated mantle magma generation temperatures and depths of magma equilibration is given in Appendix 1.

Secular changes in MgO are summarized in Fig. 1 for the four mantle domains. In this and other secular figures, median values with one standard deviation are shown for each of five age windows. Basalts from hydrated (HM) and depleted mantle (DM) show similar MgO distributions with time with medians around 8–10 wt.% MgO (Fig. 1a, b). The somewhat higher MgO values in early Archean basalts (ca. 3.8 Ga) (median = 11 wt.%) could be biased, since they come mostly from one locality, the Isua greenstone in Southwest Greenland (Appendix 1). Basalts from enriched sources (EM, Fig. 1c) also have rather similar distributions through time with median values (11–12%) greater than DM and HM types. If picrites are defined as samples with ≥12 wt.% MgO, 58 wt.% of EM basalts and 26 wt.% of HM-DM basalts are picrites. In contrast to basalts, komatiite MgO decreases through the Archean (median values drop from 27 to 25 wt.%, which may not be statistically significant), stabilizing at a median value around 22 wt.% MgO thereafter (Fig. 1d). Maximum MgO values in komatiites at 2 Ga are about 30 wt.% and the very young komatiites (≤300 Ma) range only to 28 wt.% MgO. Because of relatively few samples between 2.5 and 2 Ga, the drop in maximum MgO at the end of the Archean may not be representative. If real, however, from 2.7 to 2.0 Ga the maximum MgO decreases only from 35 to 30 wt.% rather than from 35 to 23 wt.% as suggested by Campbell and Griffiths (2014) based on fewer samples. Our results differ dramatically from those of Keller and Schoene (2012) for mafic igneous rocks. The large decline shown in their results for MgO at the end of the Archean may be due ultramafic and komatiitic rocks included in their database, which has a SiO_2 range of 43–51 wt.%.

Unlike MgO, FeO^T (total Fe as FeO) drops in DM and HM basalts with time from median values in the Archean of 10–11 to 9 wt.% in the Phanerozoic (Fig. S1a, b). In contrast, FeO^T in EM basalts and in komatiites stays rather constant with time with median values around 11 wt.% (Fig. S1c, d). Although ferropicrites and ferrokomatiites (≥15 wt.% FeO^T) are more abundant in the Archean than afterwards as pointed out by Francis et al. (1999), there is no compelling evidence for a decrease in average FeO^T in either komatiite or EM basalts with time, an observation in agreement with that of Gibson (2002). Since only a very small proportion of Archean basalts and komatiites are ferropicrites (2.5%) or ferrokomatiites (1.5%), only localized Fe-rich regions in the lower mantle may be required in the Archean, if these distributions are representative of source volumes. Mg number ($Mg^{\#}$) (MgO/(MgO + FeO^T), molecular ratio) is important in that it tracks source depletion and degree of melting, but has the disadvantage that it is also affected by fractional crystallization. Median $Mg^{\#}$ values increase in DM and HM basalts with time and especially in the last 500 Myr (Fig. S2). This is chiefly in response to the corresponding decrease in FeO^T, probably reflecting an increasingly depleted

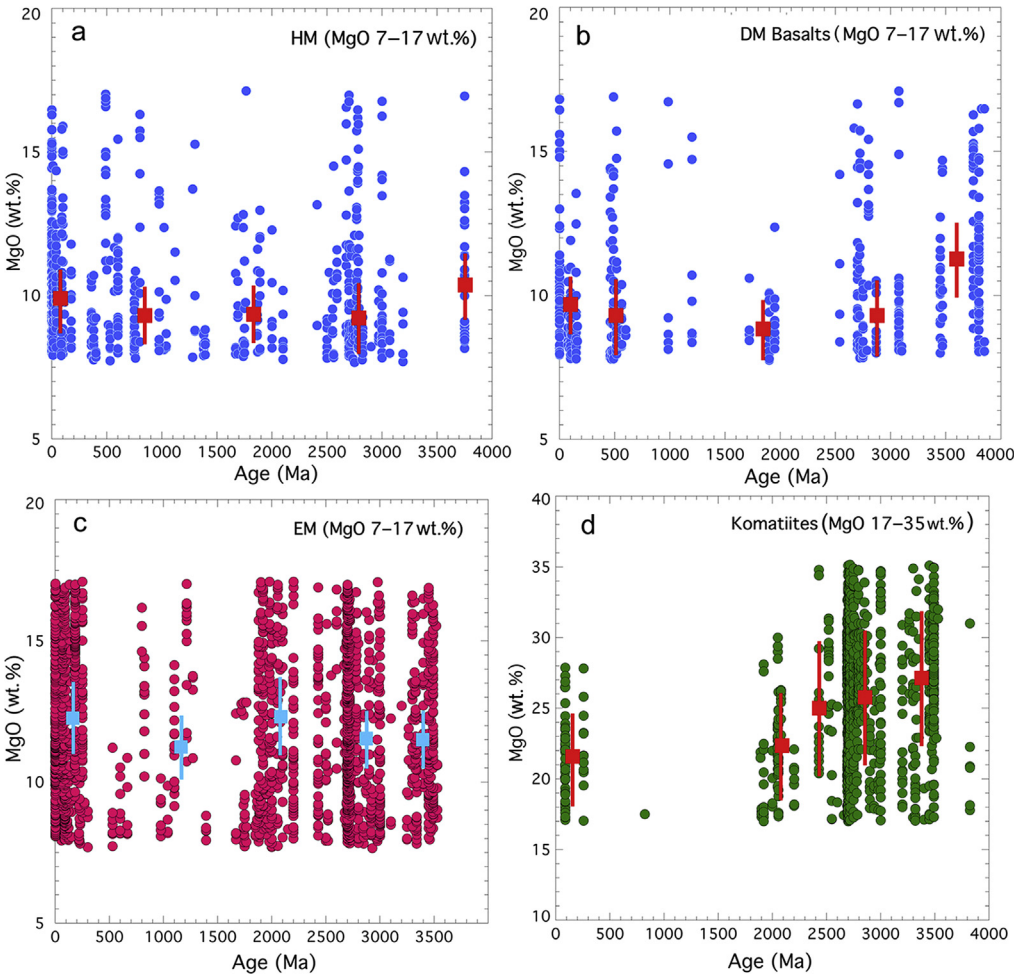

Figure 1. Secular variation in MgO in greenstone basalts (MgO 7–17 wt.%) and komatiites (MgO 17–35 wt.%). Also shown are median values and one standard deviation for the time windows specified below. (a) HM, hydrated mantle: ≤300, 1400–400, 2200–1600, 3100–2500, ≥3500 Ma; (b) DM, depleted mantle: ≤250, 1300–400, 2000-1600, 3100-2500, ≥3400 Ma; (c) EM, enriched mantle: ≤350, 1765–400, 2300–1800, 3000–2400, ≥3200 Ma; (d) komatiites: ≤350, 2200–1830, 2600–2400, 3000–2600, ≥3200 Ma.

source with time as well as a decreasing degree of melting. $Mg^{\#}$ tends to be a little lower in EM basalts in the Archean than afterwards (median of 65 in the Archean compared to 66–69 thereafter), and the decrease in $Mg^{\#}$ in komatiites at the end of the Archean reflects the corresponding drop in MgO at this time.

TiO_2 distribution is similar in DM-HM basalts through time, showing perhaps a slight increase in median values and an increase in the scatter in the last 1000 Myr (Fig. 2a, b). TiO_2 in EM basalts is relatively low in the Archean (median = 0.63–0.65 wt.%) compared to later times (median = 0.95–1.06 wt.%) and both the scatter and the median value increase in the last 500 Myr (Fig. 2c). A change in TiO_2 in komatiites comes at the end of the Archean when median values increase from 0.3–0.4 to 0.6 wt.% and remain relatively constant thereafter (Fig. 2d). The median FeO^T/TiO_2 ratio in HM-DM basalts decreases with time from ca. 16–18 in the Archean to 10–15 thereafter (Fig. S3a, b). EM basalts show a dramatic drop in FeO^T/TiO_2 from median values of 17–18 in the Archean to 8–11 thereafter, and the variation in this ratio is also greater in Archean EM basalts (Fig. S3c). The ratio also drops from median values of 26–30 in Archean komatiites to 17–18 thereafter (Fig. S3d). It is important to point out that the secular decreases in FeO^T/TiO_2 in EM basalts and komatiites are controlled chiefly by parallel increases in TiO_2 and not by changes in FeO^T. Hence, the FeO^T/TiO_2 ratio should not be used to monitor the Fe content of the lower mantle as suggested by Francis et al. (1999). CaO has similar distributions with time in DM, HM and EM basalts (median around 10 wt.%) with an increase in DM basalts in the last 250 Myr (Fig. S4a–c). In contrast, komatiites show a notable change at the end of the Archean when median CaO values increase from 6.5–7.5 to 9 wt.% (Fig. S4d). Na_2O is rather constant in HM basalts with time, but there is an increase in median values of DM basalts from 1.6–1.9 wt.% in the Archean to 2–2.5 wt.% thereafter; there is also a drop in Na_2O in DM basalts in the last 250 Myr paralleling an increase in CaO at this time (Fig. S5a, b). EM basalts show a uniform distribution in Na_2O with time (median = 1.6–1.9 wt.%) (Fig. S5c). Median values of Na_2O in komatiites are low in rocks ≥2 Ga (0.2–0.6 wt.%), but increase in komatiites <300 Ma (median = 0.8 wt.%) (Fig. S5d). Although there is considerable scatter in K_2O in basalts and komatiites, probably due to remobilization, the median values in all populations tend to remain rather constant with time. The increase in median K_2O in EM basalts after 2 Ga may be due to continental contamination of flood basalts (Fig. S6). MnO follows FeO^T and shows a decrease with time in DM and HM basalts, but remains rather constant in both EM basalts and komatiites (graph not shown). Median values of SiO_2 in DM

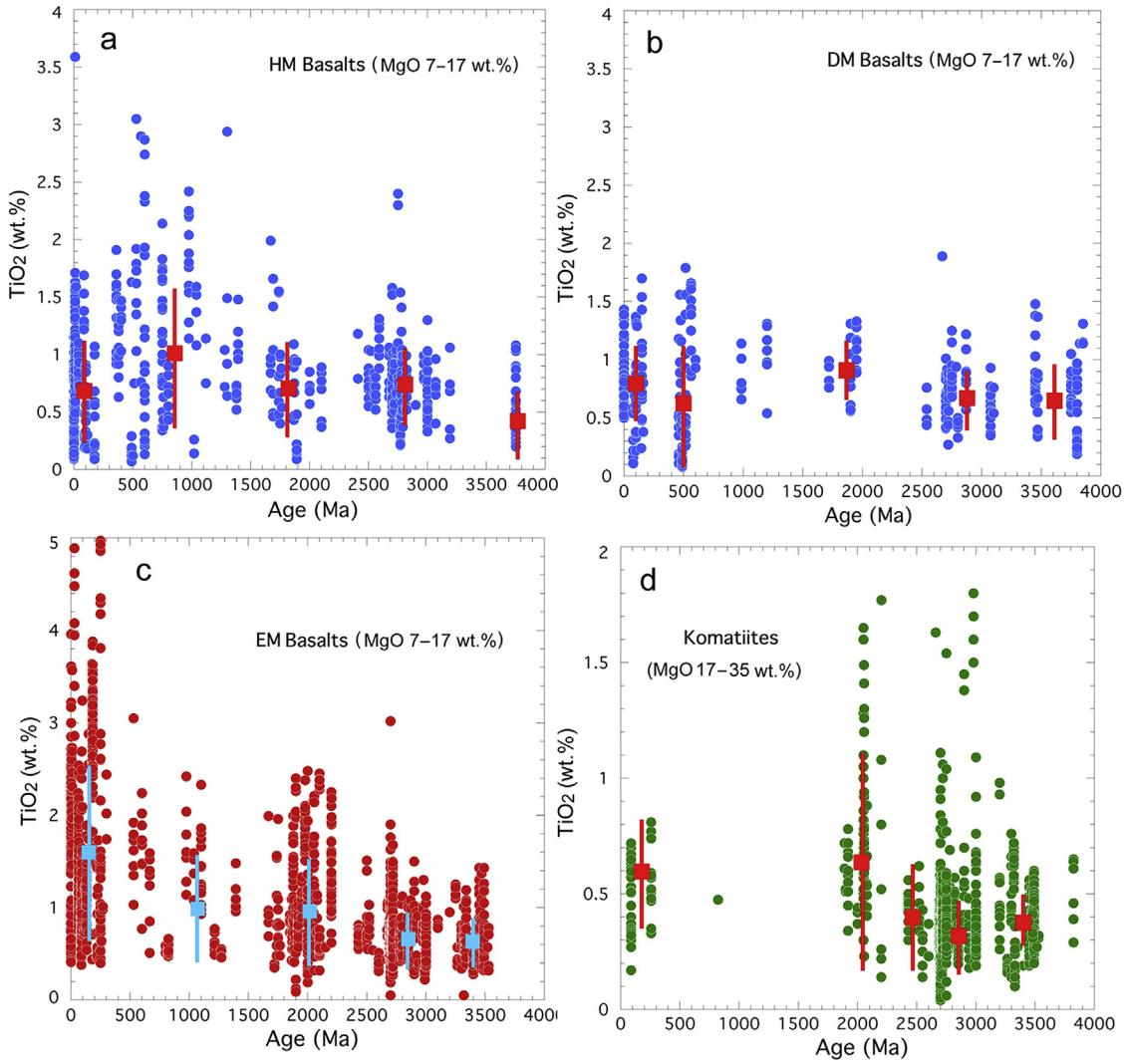

Figure 2. Secular variation in TiO_2 in greenstone basalts (MgO 7–17 wt.%) and komatiites. Other information given in Fig. 1.

and HM basalts tend to remain rather constant with time (ca. 50 wt.%), but EM basalts decrease from the Archean (median = 50–52%) to the post-Archean (median = 48–49%) (Fig. S7a–c). Komatiites have similar median SiO_2 values with time, with a possible drop in the last 300 Myr (from 47–48 to 46 wt.%) (Fig. S7d).

Al_2O_3 is rather invariable with time in DM and HM basalts (medians around 15 wt.%), although early Archean DM basalts (controlled entirely by samples from the Isua greenstone in Southwest Greenland) have a distinctly lower median (ca. 11 wt.%) (Fig. 3a, b). EM basalts have lower Al_2O_3 (10–13 wt.%) through time than DM-HM basalts (Fig. 3c). Although this difference might reflect different degrees of melting, it might also reflect different depths of melt segregation that arise because the post-2.5 Ga EM basalts include many flood basalts that could have erupted through thick lithosphere. Archean median values for EM basalts are similar to post-Archean medians, although the early Archean value is distinctly low (ca. 9.5%). Archean and Paleoproterozoic komatiite medians are low in the range of 5–7% compared to young komatiites with a median of ca. 11% (Fig. 3d). The Al_2O_3/TiO_2 ratio stays rather constant in HM-DM basalts with time (ca. median = 15–20). Median values of Al_2O_3/TiO_2 in EM basalts range from 13 to 19, with a significant decrease in the last 300 Myr that reflects the corresponding increase in TiO_2 at this time (Fig. S8a–c; Fig. 2c). Median values of this ratio in komatiites show considerable variation ranging from a low value of ca. 11 in the early Archean to a high value of ca. 20 in the late Archean and no secular trend is apparent in the data.

3.2. Mantle magma generation temperature

The first results of mantle potential temperature (T_p) (the temperature of the upper mantle extrapolated adiabatically to Earth's surface without melting) through time as calculated from mafic and ultramafic igneous rocks were reported by Abbott et al. (1994). More recent and better constrained estimates of T_p are those of Herzberg et al. (2010) using a database of 3370 samples from non-arc type greenstone basalts. The geochemical filters applied by Herzberg et al. (2010) greatly reduced the number of acceptable samples to 33. A comparison of our magma generation temperatures (T_g) for these 33 samples with the T_p results of Herzberg et al. (2010) is shown in Fig. S9. Despite differences in

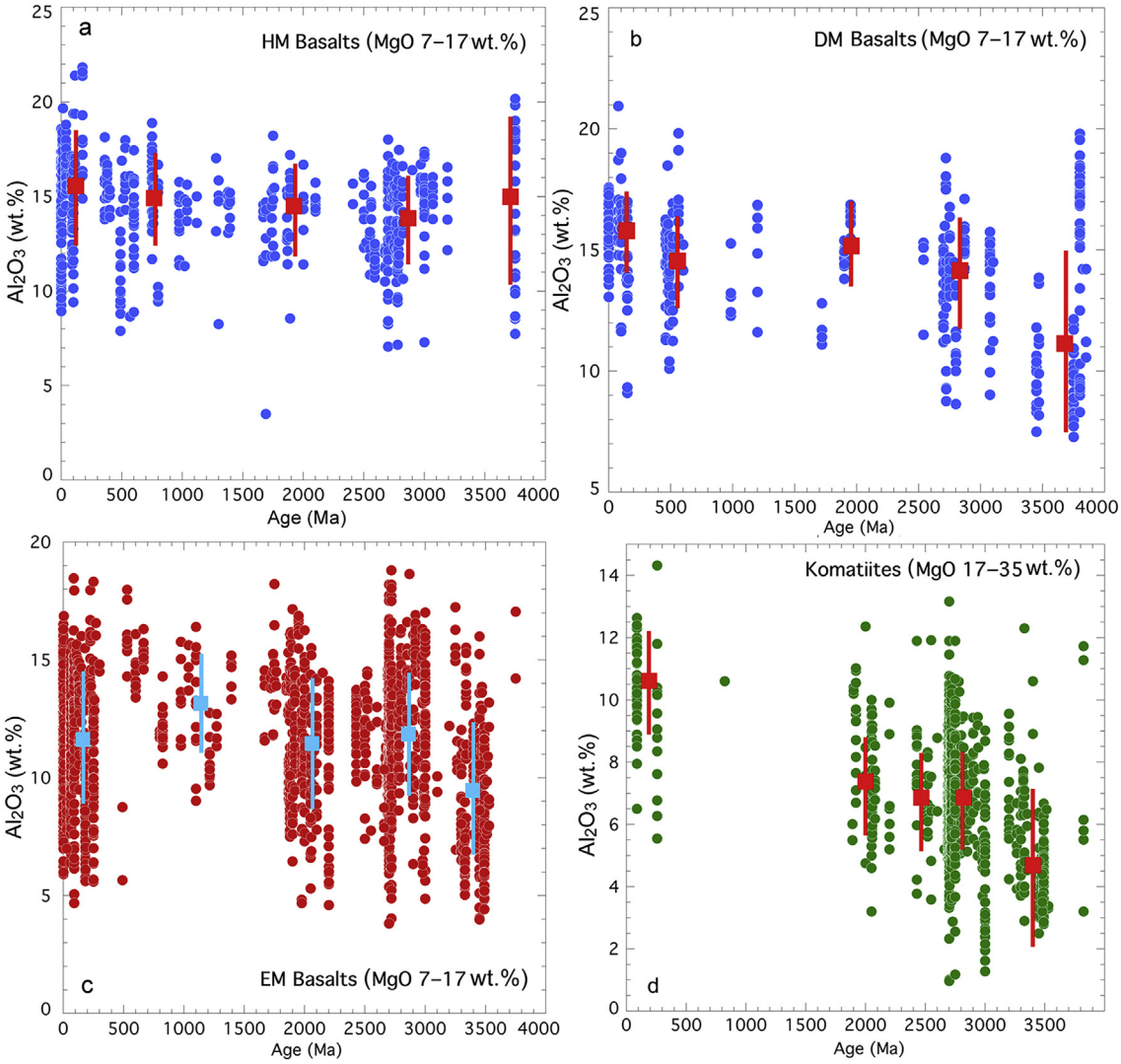

Figure 3. Secular variation in Al_2O_3 in greenstone basalts (MgO 7–17 wt.%) and komatiites. Other information given in Fig. 1.

the methods of calculating the primitive magma compositions between the two studies, the calculated T_g values are similar to the T_p values. It is important to point out that basalts from depleted (DM) and enriched mantle (EM) are not distinguished in Herzberg et al. (2010), and that 26 of the 33 samples come from enriched mantle, and thus the data distribution should not be considered as representative of the T_p of ambient mantle after 2.5 Ga.

Most T_p and T_g estimates calculated from basalts erupted at modern ocean ridges (DM type basalts) fall within an approximately 100 °C window centered about a mean value near 1350 °C (1340° Mid-Atlantic Ridge [MAR], 1360° East Pacific Rise [EPR]) (Herzberg et al., 2007; Herzberg and Asimow, 2008; Herzberg and Gazel, 2009). Mantle T_g generally varies by ≤100 °C in a given ridge segment, but this variation increases to 200–250 °C at sites where mantle plumes have an influence (Dalton et al., 2014). Results suggest that faster spreading ridges (EPR) have greater temperature variability than slower spreading ridges (MAR). The fact that HM basalts show a similar distribution of T_g to DM basalts with time, suggests that water in arc sources does not, on average, affect the T_g distribution with age and that decompression melting may be important in mantle wedges as previously suggested by Lee et al. (2009). Considering the range of T_g values in DM and HM basalts (1 σ of 60–100 °C) through time (Appendix 1), our results show a decrease in the average or median T_g with time (Fig. 4a, b), probably reflecting cooling of the mantle. This decrease begins between 2.5 and 2.0 Ga, and prior to 2.5 Ga DM and HM T_g values stay rather constant around 1500 °C.

In terms of median values, young EM basalts yield an average T_p and T_g about 150 °C higher than the ambient upper mantle temperature as recorded by DM basalts (Komiya et al., 2004; Putirka, 2005; Herzberg et al., 2007; Herzberg and Gazel, 2009), whereas in the Archean the calculated T_g from DM and EM basalts are indistinguishable (md ca. 1500 °C) (Fig. 4a–c). Intra-site variation in T_p and T_g at young EM plumes is usually the order of 80–100 °C with some sites like Hawaii showing a range up to 300 °C or more (Galapagos 1500–1700 °C; Mauna Kea 1520–1600 °C) (Herzberg and Asimow, 2008; Herzberg and Gazel, 2009). Ancient basalts from specific greenstones yield similar intra-site variations (Appendix 1). Unlike the T_g values calculated from HM and DM basalts, there is only small variation in the average or median T_g of EM basalts with time (median = 1520 °C today, about 1480 °C in the Archean, and both are identical within 1σ). Thus EM T_g remains rather constant around 1500 °C with time. This means that T_g of EM sources was indistinguishable from ambient mantle (DM) before 2.5–2.0 Ga, and during this time interval they began to diverge, which we refer to as a "Great Thermal Divergence" in the mantle. This divergence is apparent in the statistical evaluation given in Fig. 5, where the slope and standard deviation are given for a linear fit of the EM and DM data every 1 Myr for a moving 300 Myr window. The EM line may start with a slightly inverse slope that flattens with time. In any case the divergence in the two lines after 2.5 Ga is statistically significant. Post-Archean DM and HM T_g decrease by 0.059 ± 0.008 and 0.044 ± 0.005 °C/Myr, respectively (1 σ uncertainties) but EM T_g shows no significant change after the Archean. To further evaluate the statistical difference in the two trends, we performed a 2-sample Kolmorgorov-Smirnov test (Massey, 1951) on the calculated T_g for DM vs EM (Fig. 6). Again we use a 300 Myr moving window centered on the age indicated on the x axis. T_g data from the two data sets with ages within the window for the two indicated distributions are compared for statistical significance for being drawn from distinct distributions. The highest confidence levels for the two temperature distributions being different are in the last 2000 Myr with the notable exception of the time window 1500–750 Ma, which corresponds to a low sample density.

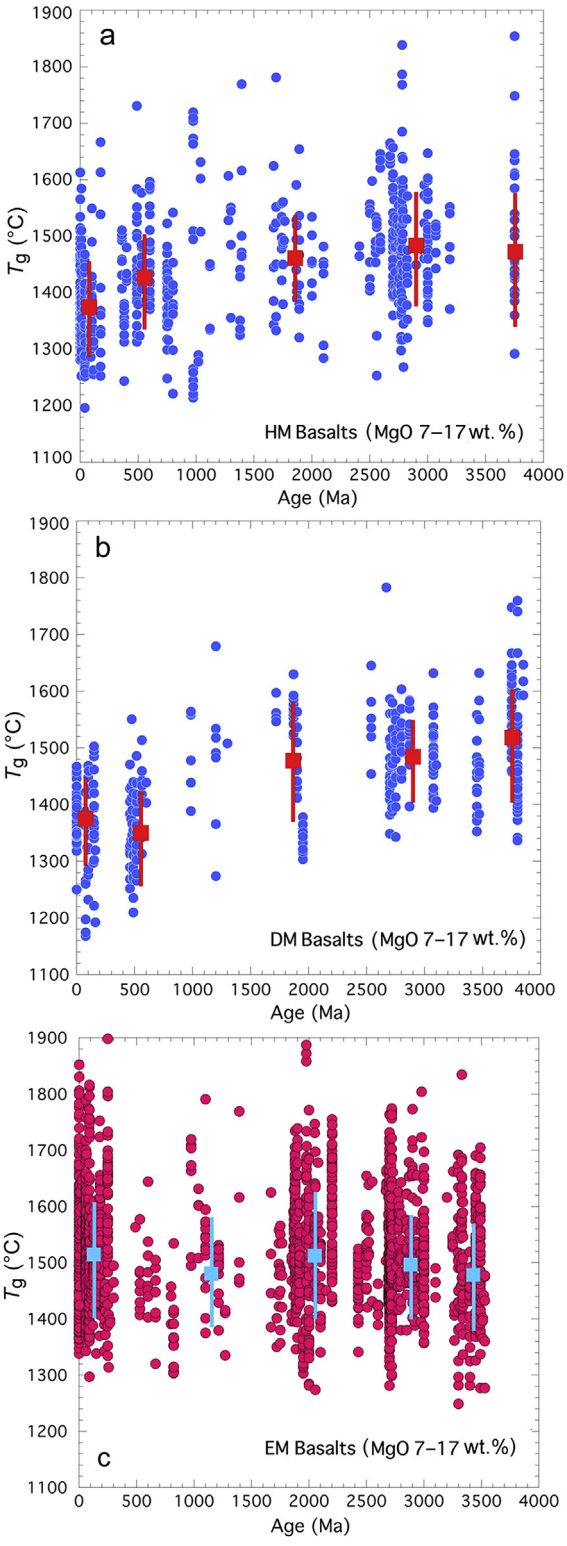

Figure 4. Secular variation in calculated mantle magma generation temperature (T_g) in greenstone basalts (MgO 7–17 wt.%). Other information given in Fig. 1.

Calculated depths of last basaltic magma equilibration show median DM and HM of 1.4 GPa (ca. 35 km) and EM at 2 GPa (ca. 65 km) (Fig. 7). The most striking feature of these results is the shallow depths of magma equilibration for all basalts and a similar

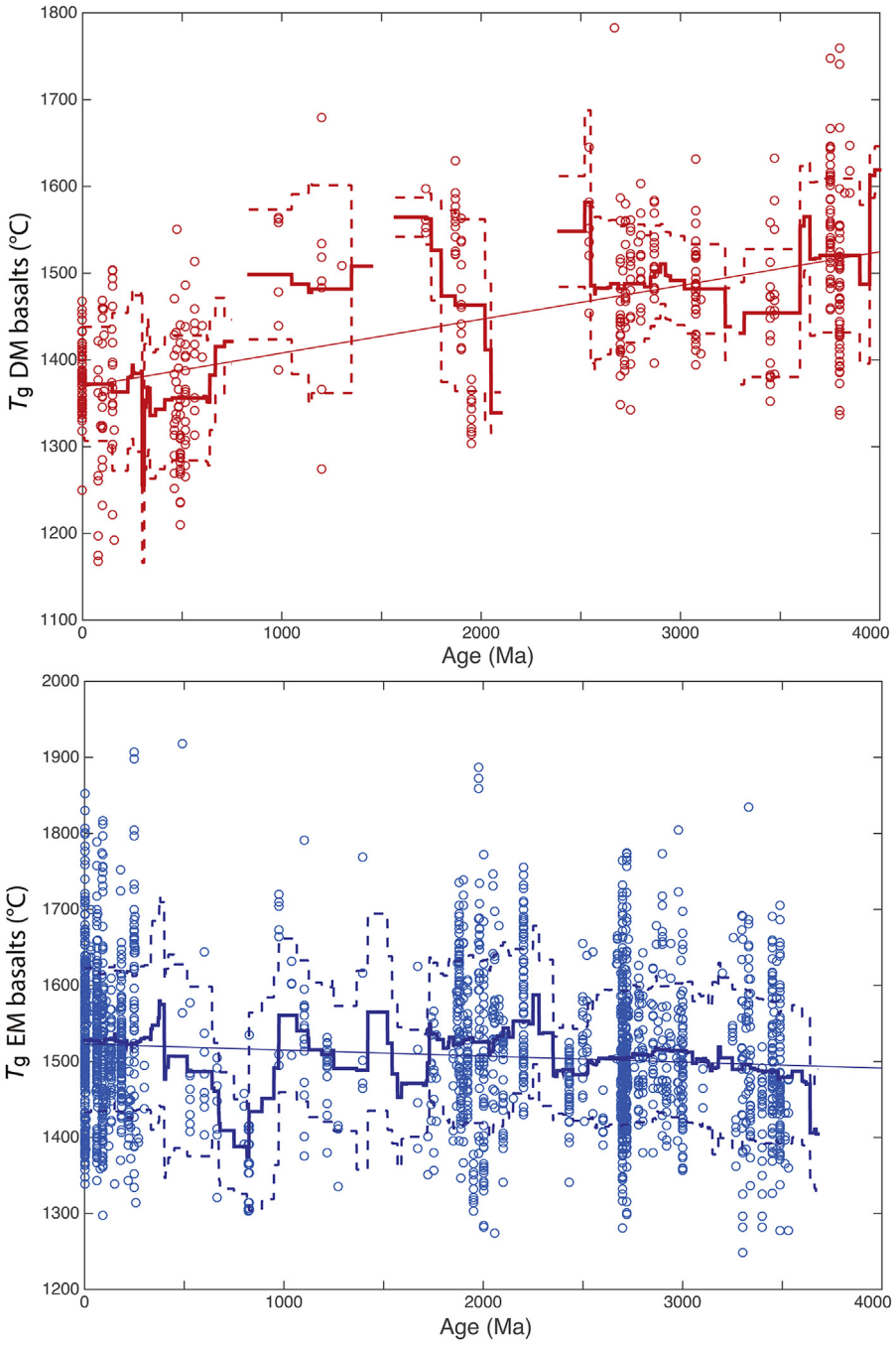

Figure 5. T_g versus age, showing moving mean (solid) and standard deviation (dashed) values calculated every 1 Myr within a moving 300 Myr window for DM and EM basalts. The solid line shows the robust (L1 normminimizing) linear trend for each data set, with the corresponding slope and its standard deviation shown in each plot.

observation was made by Lee et al. (2009). Only the EM basalts have samples that scatter to depths up to 10 GPa (ca. 300 km). Also, there is no evidence for secular change in depth with time. DM and HM depths have median values today of about 1.1 GPa ranging to 1.7 GPa in the Archean and on average they are only about 30 km shallower than EM sources. Post-Archean EM sources are slightly deeper (median = 2.1 GPa) than corresponding Archean sources (median = 1.7 GPa), and early Archean sources are even shallower (median = 1.3 GPa), but these differences are all essentially equal within 1σ of the median values.

4. Discussion

The most important observation of this paper is the recognition for the first time of a Great Thermal Divergence in the mantle beginning at the end of the Archean (Fig. 8). T_g data indicate that ambient mantle is cooled from 2.5 Ga onwards, whereas EM and KM are not significantly cooled. DM and HM both show an increase in $Mg^{\#}$ with time, especially after 2 Ga (Fig. S2a, b; Table 1), which is consistent with progressive depletion of ambient mantle with time. However, not consistent with increasing depletion are increases in

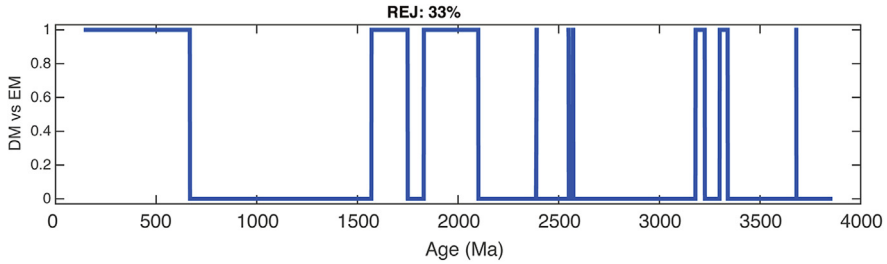

Figure 6. Two-sample Kolmorgorov-Smirnov test (Massey, 1951) for DM vs EM basalt generation temperatures (T_g) with age using a 300 Myr moving window. Time periods for which the test indicates that the two data sets arise from differing distributions (at the 95% confidence level) are indicated with test values of one, and periods that are not different at this significance level are indicated with test values of zero. Time windows are advanced in steps of 1 Myr. The REJ percentage indicates the percentage of windows where the windowed dates appear to come from different distributions (again at 95% confidence).

Ti and Na with time in DM, and these trends may reflect decreasing degrees of melting. Ti is incompatible and Na is contained largely in clinopyroxene, so both elements should be more enriched in the melt at smaller degrees of melting.

If EM basalts come dominantly from mantle plumes today, what is the history of plumes as we go back in time? If as Korenaga (2008) suggested, the core heat flux was lower prior to 2.5 Ga, plume activity may have been less vigorous than afterwards. However, two lines of evidence suggest that pre-2.5 Ga EM basalts did not come from plume sources: (1) prior to this time, EM and DM basalts have similar compositions and calculated Tgs, which makes a buoyancy force for rising mantle plumes less obvious, and (2) there are compositional differences between pre- and post-2.5-Ga EM basalts (Figs. 1–4). There are three compositional differences between pre- and post-2.5-Ga EM basalts: TiO_2 and possibly $Mg^{\#}$ are higher and SiO_2 is lower in post-2.5-Ga EM (Fig. 2c; Figs. S2 and S7; Table 1). The higher SiO_2 in Archean EM may reflect a greater contribution of clinopyroxene to the melts. The increase in TiO_2 in EM basalts in the last 2.5 Gyr (especially in the last 500 Myr) supports a TiO_2-rich mantle source. Could it be that recycling of oceanic crust in the last 2.5 Gyr into the EM source regions of mantle plumes selectively introduced TiO_2 into these sources? Supporting this possibility is a parallel enrichment in Nb in post-2.5-Ga EM basalts (Fig. S10). Both Ti and Nb in oceanic crust are preferentially recycled into the mantle at subduction zones. An increase in Ti (and Nb, not shown) in post-2.5-Ga komatiites also may be explained by deep crustal recycling (Fig. 2d; Appendix 1). The bottom line is that prior to 2.5 Ga, EM sources were not the same as those afterwards. This may also account for an ongoing difficulty in distinguishing DM and EM basalts in the Archean based on geological and incompatible trace element characteristics (Condie, 1994, 2003, 2015).

The Al_2O_3/TiO_2 ratio is commonly used to classify komatiites since it is sensitive to garnet in the residue, which records the depth of magma equilibration prior to eruption (Arndt et al., 2008). Our results show no consistent trend in this ratio with time (Fig. S8d). Unlike Robin-Popieul et al. (2012), we see no evidence for a drop in proportion of Al-depleted komatiites through time and thus no progressive decrease in the depth of komatiite generation with time. In fact, the proportion of Al-depleted types is actually higher in 2.2–1.9 Ga komatiites than it is in those >2.5 Ga (Fig. S8d; Table 2). The anomalously low Al_2O_3 and Al_2O_3/TiO_2 in early Archean (3.5 Ga) komatiites (and in EM basalts) chiefly reflects data from the Barberton greenstone in South Africa (Robin-Popieul et al., 2012). These low values may result from majorite garnet fractionation, reflecting greater depths of the beginning of melting. Al-undepleted komatiites dominate in both the Archean and post-Archean (60–70%; Table 2). Our results suggest that young komatiites (<300 Ma) are almost exclusively undepleted and enriched types, reflecting shallower depths of melting than for komatiites ≥1.9 Ga. The CaO/Al_2O_3 ratio has also been used to monitor the depth of komatiite generation with time (Herzberg, 1995). We see no evidence for a gradual decrease in the CaO/Al_2O_3 ratio in komatiites with time; there is a suggestion, however, of a drop in this ratio from the early to the late

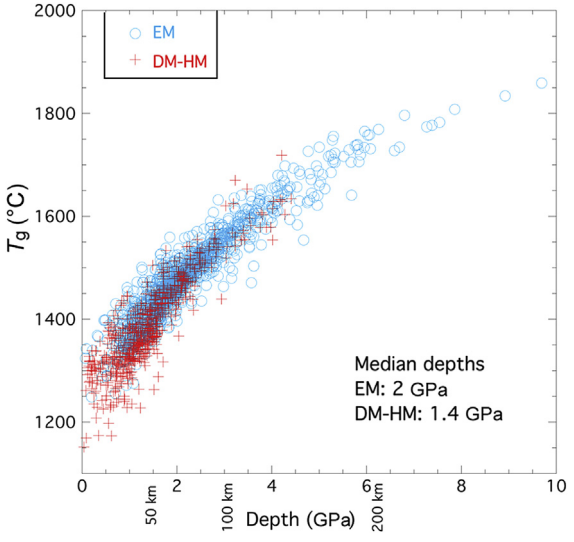

Figure 7. Calculated mantle magma generation temperature (T_g) versus depth of last magma equilibration. DM-HM, EM, depleted-hydrated, enriched mantle. GPa, gigapascal.

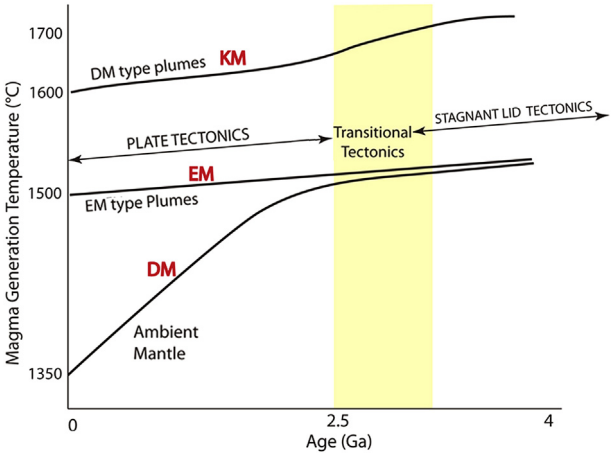

Figure 8. Summary showing the "Great Thermal Divergence" between depleted (DM) and enriched (EM) mantle beginning at 2.5–2.0 Ga. KM (komatiite) T_g from Herzberg et al. (2007) and Herzberg and Asimow (2008).

Table 1
Summary of geochemical, T_g and depth changes for 3.8 Gyr.

	Decrease	Increase	No change
Komatiites	Mg, $Mg^{\#}$, Fe/Ti, Ca/Al	Ti, Al, Ca, Na	GPa, Fe, Si, K, Al/Ti, Mn
EM basalts	Fe/Ti, Si	Ti, $Mg^{\#}$	Fe, Al, Ca, Tg, K, Mg, GPa, Mn, Na, Al/Ti
DM and HM basalts	T_g, Fe, Mn, Fe/Ti	$Mg^{\#}$, Na, Ti	Si, Mg, K, Al, Ca, GPa, Al/Ti

Table 2
Distribution of komatiite types with age (Al-depleted Al_2O_3/TiO_2 <13; Al-undepleted 13–25; Al-enriched >25).

	Archean	%	Post-Archean	%
Al-depleted	222	22	52	31
Al-undepleted	693	68	97	58
Al-enriched	108	10	19	11

Archean (Appendix 1). Almost all komatiites of all ages fall in the low-TiO_2 field on the TiO_2–MgO graph of Parman and Gove (2005) (Fig. S11) indicating they come from depleted mantle sources. On the SiO_2–MgO graph (Parman and Gove, 2005) (Fig. S12), most komatiites of all ages fall in the anhydrous melting field (88%) suggesting that water did not play a role in their production. The remaining 12% of the samples that fall in the hydrous melting field are mostly Archean in age. The near absences of high SiO_2 komatiites as well as the oxidation state of Fe in komatiites also support a dry rather than wet mantle source (Berry et al., 2008; Lee et al., 2009).

The drop in MgO between the early and late Archean may or may not be real since most of the 3500 Ma samples come from only one site: the Barberton greenstone in South Africa (Fig. 1d). If this source is anomalously enriched in MgO, it may not be typical of Archean komatiite sources. In any case, our results do not support a sudden large drop in MgO at the end of the Archean in komatiite sources (mean, median or maximum values) as suggested by studies with fewer samples (Condie and O'Neill, 2010; Campbell and Griffiths, 2014). Thus, there is no motivation for complex models to explain a sudden drop in komatiite source temperatures. If real, the overall decrease in MgO during the Archean probably reflects a decrease in degree of melting in response to cooling of the mantle. The increases in Ti, Al, Ca and Na and decrease in $Mg^{\#}$ in komatiites at the end of the Archean (Table 1) may reflect a falling degree of melting with increasing amounts of garnet and clinopyroxene contributing to the melts. Prior to 2.5 Ga, high degrees of melting removed these minerals from the source. A similar conclusion was reached by Gibson (2002). Recycling of oceanic crust into the deep mantle after the Archean may also have contributed to enrichment of Ti, Al, Ca and Na in komatiite sources, as suggested above for post-Archean EM sources. Although previous studies have argued for recycling into the deep mantle by 3.8–3.5 Ga based on isotopic evidence (Turner et al., 2014; Blichert-Toft et al., 2015), such early recycling appears not to have affected major elements in derivative basalts.

Our results clearly show a Great Thermal Divergence in the history of the mantle. Before 2.5 Ga, thermal regimes in ambient mantle (DM, HM) and enriched mantle (EM) are indistinguishable in terms of thermal characteristics, whereas after this time ambient mantle progressively decreases in T_g, probably due to mantle cooling (Fig. 8). It is important to emphasize here that tracking these types of mantle into the Archean–Hadean does not necessarily equate with tracking plate tectonics into these times, because these types of mantle also could exist in a planetary stagnant lid regime (Condie, 2015). The increase in $Mg^{\#}$ and decrease in Fe and Mn in DM and HM basalts after 2.5 Ga reflects some combination of growing depletion and cooling of ambient mantle with time. Complicating this interpretation, however, is the fact that fractional crystallization also affects the $Mg^{\#}$. Secular increases in Ti and Na in DM and HM basalts may be related to a smaller degree of melting with time. Different depths of melt segregation may also affect the EM basalts, many of which have come through continental lithosphere, at least those younger than 2.5 Ga. These trends are also consistent with high rates of extraction of continental crust between 3 and 2 Ga as reflected by Hf model ages (Dhuime et al., 2012) and on ^{40}Ar model ages (Pujol et al., 2013). The fact that Al and Ca do not track mantle depletion may be due to their being hosted by residual garnet in the source.

Why was cooling of ambient mantle delayed until after the Archean? Two factors may have contributed to this delay: (1) radiogenic heat sources were more important in the Archean and Hadean, and (2) cooling was enhanced by the onset and propagation of plate tectonics with descending slabs increasing the mantle cooling rate (Condie et al., 2015). Plate tectonics may have begun episodically around 3 Ga, as geochemical and geological observations and geodynamic modeling suggest (Moyen and van Hunen, 2012), followed by widespread propagation between 2.5 and 2.0 Ga (O'Neill et al., 2007; Condie and O'Neill, 2010). A dramatic increase in abundance of basalts showing DM and EM chemical characteristics and a corresponding decrease in those showing primitive mantle characteristics after 2.5 Ga supports such a model (Condie, 2015). Before 2.5 Ga, DM and EM basalts may have been derived from an undifferentiated or well-mixed mantle sources similar in composition to calculated primitive mantle. After this time EM basalts appear to have come from EM type plumes, which could now propagate upwards to the base of the lithosphere due to cooling ambient mantle and the corresponding increase in thermal contrast necessary for them to rise (Fig. 8). Before 2.5 Ga, and only DM type (high-temperature) mantle plumes, which gave rise to komatiites and associated basalts, made it to the base of the lithosphere. After 2.5 Ga, the DM type plume source was rarely active in producing plumes that made it to the base of the lithosphere.

5. Conclusions

Greenstone basalts can be used to estimate mantle magma generation temperatures through time and thus to track the thermal history of the mantle. Based on modern mantle compositional and thermal domains, four types of mantle can be traced into the Archean: depleted (DM), hydrated (HM), enriched (EM) and mantle from which komatiites are derived (KM). Prior to 2.5 Ga, DM, HM and EM have indistinguishable thermal histories, whereas beginning at 2.5–2.0 Ga a Great Divergence occurs in mantle magma generation temperatures between DM-HM and the EM mantle types. DM and HM mantle fall in T_g, whereas EM maintains high values after this time. The indistinguishable thermal regimes, yet different compositional characteristics of DM-HM and EM basalts before 2.5–2.0 Ga require different mantle sources for EM basalts before and after this time. Before 2.5 Ga, DM and EM basalts may have been derived from an undifferentiated or well-mixed mantle source similar in composition to calculated primitive mantle. After 2.5 Ga, EM basalts were probably produced dominantly in mantle plumes that were sourced in enriched mantle. The dramatic change in mantle thermal regimes beginning after the Archean, reflected by temporal trends in mantle magma generation temperature, corresponds to a possible transition in Earth's tectonic regime from stagnant lid to plate tectonics. If so, this "Great Thermal Divergence" between depleted and enriched mantle beginning at this time may reflect enhanced cooling of the mantle by subduction.

Only after 2.5 Ga was the thermal contrast between EM type plumes and ambient mantle sufficient for these plumes to survive to the base of the lithosphere where partial melting gave rise to EM basalts. In contrast, KM type plumes with high temperatures that give rise to komatiites and associated basalts, dominated in the Archean and were produced only infrequently after this time.

Acknowledgments

We acknowledge Cin-Ty Lee and Claude Herzberg for in-depth reviews and discussion of the manuscript, which led to important revisions and clarifications. Jeroen van Hunen acknowledges funding from the European Research Council (ERC StG 279828).

Appendix A. Supplementary data

Supplementary data related to this article can be found at http://dx.doi.org/10.1016/j.gsf.2016.01.006.

References

Abbott, D.H., Burgess, L., Longhi, J., Smith, W.H.F., 1994. An empirical thermal history of the Earth's upper mantle. Journal of Geophysical Research 99, 13,835–13,850.
Arndt, N.T., Lesher, C.M., Barnes, S.J., 2008. Komatiite. Cambridge University Press, Cambridge, U. K.
Berry, A.J., Danyushevsky, L.V., O'Neill, H.S.C., Newville, M., Sutton, S.R., 2008. Oxidation state of iron in komatiitic melt inclusions indicates hot Archaean mantle. Nature 455, 960–964.
Blichert-Toft, J., Arndt, N.T., Wilson, A., Coetzee, G., 2015. Hf and Nd isotope systematics of early Archean komatiites from surface sampling and ICDP drilling in the Barberton Greenstone Belt, South Africa. American Mineralogist 100, 2396–2411.
Campbell, I.H., 2002. Implications of Nb/U, Th/U and Sm/Nd in plume magmas for the relationship between continental and oceanic crust formation and the development of the depleted mantle. Geochimica et Cosmochimica Acta 66, 1651–1661.
Campbell, I.H., Griffiths, R.W., 2014. Did the formation of D″ cause the Archaean-Proterozoic transition? Earth and Planetary Science Letters 388, 1–8.
Campbell, I.H., Griffiths, R.W., Hill, R.I., 1989. Melting in an Archean mantle plume: heads it's basalts, tails it's komatiites. Nature 339, 697–699.
Condie, K.C., 1994. Greenstones through time. In: Condie, K.C. (Ed.), Archean Crustal Evolution. Elsevier, Amsterdam, pp. 85–120.
Condie, K.C., 2003. Incompatible element ratios in oceanic basalts and komatiites: tracking deep mantle sources and continental growth rates with time. Geochemistry, Geophysics, Geosystems 4 (1), 1005. http://dx.doi.org/10.1029/2002GC000333.
Condie, K.C., 2015. Changing tectonic settings through time: indiscriminate use of geochemical discriminant diagrams. Precambrian Research 266, 587–591.
Condie, K.C., O'Neill, C., 2010. The Archean-Proterozoic boundary: 500 My of tectonic transition in Earth history. American Journal of Science 310, 775–790.
Condie, K.C., Davaille, A., Aster, R.C., Arndt, N., 2015. Upstairs-downstairs: supercontinents and large igneous provinces, are they related? International Geology Review 57 (11-12), 1341–1348.
Dalton, C.A., Langmuir, C.H., Gale, A., 2014. Geophysical and geochemical evidence for deep temperature variations beneath mid-ocean ridges. Science 344, 80–83.
Davies, G.F., 2007. Thermal Evolution of the Mantle, Treatise on Geophysics, vol. 9. Elsevier, pp. 197–216.
Dhuime, B., Hawkesworth, C.J., Cawood, P.A., Storey, C.D., 2012. A change in the geodynamics of continental growth 3 billion years ago. Science 335, 1334–1336.
Francis, D., Ludden, J., Johnston, R., Davis, W., 1999. Picrite evidence for more Fe in Archean mantle reservoirs. Earth and Planetary Science Letters 167, 197–213.
Gibson, S.A., 2002. Major element heterogeneity in Archean to recent mantle plume starting-heads. Earth and Planetary Science Letters 195, 59–74.
Hart, S.R., 1988. Heterogeneous mantle domains: signatures, genesis and mixing chronologies. Earth and Planetary Science Letters 90, 273–296.
Herzberg, C., 1995. Generation of plume magmas through time: an experimental perspective. Chemical Geology 126, 1–16.
Herzberg, C., Asimow, P.D., 2008. Petrology of some oceanic island basalts: PRIMELT2.XLS software for primary magma calculation. Geochemistry, Geophysics, Geosystems 8, Q09001. http://dx.doi.org/10.1029/2008GC002057.
Herzberg, C., Gazel, E., 2009. Petrological evidence for secular cooling in mantle plumes. Nature 458, 619–622.
Herzberg, C., Asimow, P.D., Arndt, N., Niu, Y., Lesher, C.M., Fitton, J.G., Cheadle, M.J., Saunders, A.D., 2007. Temperatures in ambient mantle and plumes: constraints from basalts, picrites and komatiites. Geochemistry, Geophysics, Geosystems 8, Q02006. http://dx.doi.org/10.1029/2006GC001390.
Herzberg, C., Condie, K.C., Korenaga, J., 2010. Thermal history of the Earth and its petrological expression. Earth and Planetary Science Letters 292, 79–88.
Hofmann, A.W., 1988. Chemical differentiation of the earth: the relationship between mantle, continental crust, and oceanic crust. Earth and Planetary Science Letters 90, 297–314.
Hofmann, A.W., 1997. Mantle geochemistry: the message from oceanic volcanism. Nature 385, 219–229.
Hoink, T., Lenardic, A., Jelinek, A.M., 2013. Earth's thermal evolution with multiple convection modes: a Monte-Carlo approach. Physics of the Earth and Planetary Interiors 221, 22–26.
Keller, C.B., Schoene, B., 2012. Statistical geochemistry reveals disruption in secular lithospheric evolution about 2.5 Gyr ago. Nature 485, 490–493.
Komiya, T., Maruyama, S., Hirata, T., Yurimoto, H., Nohda, S., 2004. Geochemistry of the oldest MORB and OIB in the Isua Supracrustal Belt, southern West Greenland: implications for the composition and temperature of early Archean upper mantle. The Island Arc 13, 47–72.
Korenaga, J., 2008. Plate tectonics, flood basalts and the evolution of Earth's oceans. Terra Nova 20 (6), 419–439.
Korenaga, J., 2013. Initiation and evolution of plate tectonics on Earth: theories and observations. Annual Reviews Earth and Planetary Sciences 41, 117–151.
Labrosse, S., Jaupart, C., 2007. Thermal evolution of the Earth: secular changes and fluctuations of plate characteristics. Earth and Planetary Science Letters 260, 465–481.
Lee, C.-T., Luffi, P., Plank, T., Dalton, H., Leeman, W.P., 2009. Constraints on the depths and temperatures of basaltic magma generation on Earth and other terrestrial planets using new thermobarometers for mafic magmas. Earth and Planetary Science Letters 279, 20–33.
Lee, C-T., Bachmann, O., 2014. How important is the role of crystal fractionation in making intermediate magmas? Insights from Zr and P systematics. Earth and Planetary Science Letters 393, 266–274.
Massey, F.J., 1951. The Kolmogorov-Smirnov test for goodness of fit. Journal of the American Statistical Association 46 (253), 68–78.
Moyen, J.-F., van Hunen, J., 2012. Short-term episodicity of Archaean plate tectonics. Geology 40 (5), 451–454.
Nakagawa, T., Tackley, P.J., 2012. Influence of magmatism on mantle cooling, surface heat flow and Urey ratio. Earth and Planetary Science Letters 329–330, 1–10.
O'Neill, C.O., Lenardic, A., Moresi, L., Torsvik, T.H., Lee, C.-T.A., 2007. Episodic Precambrian subduction. Earth and Planetary Science Letters 262, 552–562.
Parman, S.W., Gove, T.L., 2005. Komatiites in the plume debate. Geological Society of America Special Paper 388, 249–256.
Pujol, M., Bernard, M., Burgess, R., Turner, G., Philippots, P., 2013. Argon isotopic composition of Archaean atmosphere probes early Earth geodynamics. Nature 498, 87–90.
Putirka, K.D., 2005. Mantle potential temperatures at Hawaii, Iceland, and the mid-ocean ridge system, as inferred from olivine phenocrysts: evidence for thermally driven mantle plumes. Geochemistry, Geophysics, Geosystems 6 (5), Q05L08. http://dx.doi.org/10.1029/2005GC000915.
Robin-Popieul, C.C.M., Arndt, N., Chauvel, C., Byerly, B.R., Sobolev, A.V., Wilson, A., 2012. A new model for Barberton komatiites: deep critical melting with high melt retention. Journal of Petrology 53, 2191–2229.
Stracke, A., 2012. Earth's heterogeneous mantle: a product of convection-driven interaction between crust and mantle. Chemical Geology 330–331, 274–299.
Turner, S., Rushmer, T., Reagan, M., Moyen, J.-F., 2014. Heading down early on? Start of subduction on Earth. Geology 42, 139–142.
Van Hunen, J., Moyen, J.-F., 2012. Archean subduction: fact or fiction? Annual Reviews Earth and Planetary Sciences 40, 195–219.

Kent C. Condie Degrees: BS Geology (1959) and MA mineralogy (1960), University of Utah; PhD, University of California, San Diego, geochemistry (1965). Kent Condie is professor of geochemistry at New Mexico Institute of Mining and Technology, Socorro, NM where he has taught since 1970. Prior to that time he was at Washington University in St. Louis, MO (1964–1970). Textbook, **Plate Tectonics and Crustal Evolution,** which is widely used in upper division and graduate courses in the Earth Sciences, was first published in 1976 and has gone through four previous editions. In addition Condie has written a beginning historical geology textbook with coauthor Robert Sloan, **Origin and Evolution of Earth** (Prentice-Hall, 1998), an advanced textbook, **Mantle Plumes and Their Record in Earth History** (Cambridge University Press, 2001), and a research treatise, **Archean Greenstone Belts** (Elsevier, 1981). His most recent book, written as an upper division/graduate textbook, is **Earth as an Evolving Planetary System** has gone through three editions (Elsevier, 2005; 2011; 2016). He also has edited two books, **Proterozoic Crustal Evolution** (Elsevier, 1992) and **Archean Crustal Evolution** (Elsevier, 1994). His CD ROM, **Plate Tectonics and How the Earth Works** is widely used in upper division Earth Science courses in the United States and Europe. Condie's research, primarily dealing with the origin and evolution of continents and the early history of the Earth, has over the years been sponsored chiefly by the U. S. National Science Foundation. He is author or co-author of over 750 articles published scientific journals.

Richard C. Aster is Professor of Geophysics and Department Head in the Department of Geosciences at Colorado State University. Degrees: BS in Electrical Engineering and additional major in Physics at University of Wisconsin (1983), MS, Geophysics, University of Wisconsin-Madison (1986), Ph.D. Earth Sciences, University of California, San Diego (1991). Aster has long-standing research interests in earthquake, volcano, Antarctic and structural/imaging seismology, as well as data analysis and inverse methods. He has over 120 authored and co-authored publications, arising from research supported by the U.S. National Science Foundation, U.S. Department of Energy, U.S. Geological Survey, and other sponsors. He is the author (with B. Borchers and C. Thurber) of a widely used textbook in geophysical and mathematical modeling, **Parameter Estimation and Inverse Problems**, second edition (Aster et al., Elsevier, 2013).

Dr Jeroen van Hunen is a Reader in Computational Geoscience at Durham University, UK. His main expertise is in large-scale geodynamics, with a particular interest in subduction dynamics, continental collision, mantle convection, intra-plate volcanism, craton stability, plate-mantle interaction, early Earth dynamics, and continental crust formation. He has published over 50 peer-reviewed articles in international recognized journals.